Journal of Radioanalytical and Nuclear Chemistry

Title page

Names of the authors: Alexandra Espriu-Gascon[1], Jordi Llorca[1], Montserrat Domínguez[1], Javier Giménez[1], Ignasi Casas[1], Joan de Pablo[1,2]

Title: Oxidation by H_2O(g) in the presence of H_2(g) of UO_2 doped with Pd nanoparticles

Affiliation(s) and address(es) of the author(s): 1. Barcelona Research Center for Multiscale Science and Engineering, Universitat Politècnica Catalunya-Barcelona Tech, Av. Eduard Maristrany, 10-14, 08930. 2. Fundació CTM Centre Tecnològic, Plaça de la Ciència 2, E-08243 Manresa

E-mail address of the corresponding author: francisco.javier.gimenez@upc.edu

Journal of Radioanalytical and Nuclear Chemistry

Oxidation by H_2O(g) in the presence of H_2(g) of UO_2 doped with Pd nanoparticles

Alexandra Espriu-Gascon[1], Jordi Llorca[1], Montserrat Domínguez[1], Javier Giménez[1], Ignasi Casas[1], Joan de Pablo[1,2]

1. Barcelona Research Center for Multiscale Science and Engineering, Universitat Politècnica Catalunya-Barcelona Tech, Av. Eduard Maristrany, 10-14, 08930

2. Fundació CTM Centre Tecnològic, Plaça de la Ciència 2, E-08243 Manresa

Abstract

This work studies the influence of epsilon particles and metallic precipitates, simulated through the deposition of Pd nanoparticles on non-irradiated UO_2, on the oxidation of the spent nuclear fuel (SNF). The presence of Pd nanoparticles favored the reduction by hydrogen of oxidized uranium phases located on the UO_2 surface, decreased the oxidation of the UO_2 by H_2O in the absence of hydrogen, and, in the presence of hydrogen and water vapor, no oxidation of the UO_2 by water was detected, contrasting with experiments without Pd nanoparticles.

Keywords

Epsilon particles; metallic particles; spent nuclear fuel; palladium nanoparticles; molecular hydrogen; UO_2 oxidation

Introduction

Redox conditions in the near-field of the spent nuclear fuel (SNF) in a High-Level Nuclear Waste Repository are crucial, mainly because of the higher solubility of U(VI)-solid phases compared with U(IV)-solid phases. The oxidation of UO_2, the main component of the SNF, would involve a higher dissolution of the fuel and a higher release of radionuclides to the groundwaters after the canister failure.

Redox conditions will depend on the formation of oxidizing and reducing species by different processes such as radiolysis of water and canister corrosion. In addition, water vapor might be also present in the near-field due to residual water from the cooling pools in the nuclear power plants or from the evaporation of groundwaters at the temperature of the repository [1–3]. The presence of water vapor is of particular importance because it was demonstrated to enhance the oxidation rate of the SNF matrix at ambient temperature [4,5]

On the other hand, one of the main reducing species formed in the near-field of the SNF is molecular hydrogen from water radiolysis and the corrosion of the metallic canister [6,7]. Hydrogen might react with oxidizing species formed in the near-field hindering the oxidation of UO_2. For example, the consumption of hydrogen peroxide in contact with hydrogen was observed at hydrogen partial pressures between 10 and 48 bar [8]. In addition, previous results of the extent of UO_2 oxidized by water vapor showed that in the presence of hydrogen the percentage of U(IV) in the surface of UO_2 subjected to oxidation by water vapor increased from 7% to 64% at 350 ºC [9].

The role of molecular hydrogen hindering the oxidation of the UO_2 could be even more important if the presence of metallic precipitates and epsilon particles in the SNF is considered [10,11]. ϵ-particles are defined as metallic precipitates of noble metals (such as Au, Ag, Pd, Pt, Ru, Rh and Mo) and are believed to function as catalyzers of the reduction reactions by hydrogen [10,12–14], resulting in less oxidizing conditions near the fuel. These particles and precipitates are expected to have an important role on the oxidative dissolution of the SNF.

The aim of the present work is to find out the impact of epsilon particles and metallic precipitates on the redox processes involving hydrogen and water vapor in the near-field of the SNF. In this sense, epsilon particles and metallic precipitates in the SNF were simulated by depositing Pd nanoparticles on UO_2 powder, and the extent of oxidation of Pd-doped UO_2 by water vapor in the presence of hydrogen was determined by X-ray Photoelectron Spectroscopy (XPS) measurements of the solid surface at different temperatures.

Experimental

Preparation of UO_2 doped with Pd nanoparticles

Three samples of non-irradiated UO_2 powdered pellets from ENUSA (Empresa Nacional del Uranio S.A., Spain) were used in this study. One of the samples was not doped with Pd nanoparticles. The other two samples contained 0.5 % of Pd (simulating a SNF with epsilon particles) and 1.5 % of Pd (simulating the formation of metallic precipitates in a high-burnup fuel sample). The percentages of Pd deposited were calculated considering the inventories of a SNF with 60 $MWd \cdot kg_U^{-1}$ burn-up [15].

The doping procedure and the sample characterization was the same than in Espriu-Gascon et al. [16]. Briefly, $PdCl_2$(s) was dissolved into 0.5% of HCl, the resulting solution was added drop by drop to a powder sample of UO_2 until the solid was saturated with the solution. Then, the solid was dried in the oven at 60 ^{0}C. These last two steps were repeated until all the Pd/HCl solution was located on the UO_2 powder. Afterwards, the solid was heated at 350 ^{0}C for 24 hours. The characterization of the solid obtained at the end of the deposition showed the successful incorporation of Pd nanoparticles to UO_2 [23].

After the deposition of the Pd nanoparticles, the three samples were separately compressed to obtain three pellets with 13 mm diameter and 1 mm thickness. The compressed pellets were placed on the XPS sample holder and introduced into the XPS platform.

XPS measurements

XPS was used to determine the uranium oxidation state in the surface of the solids at the end of the experiments. XPS spectra were recorded in a SPECS system equipment. The anode was an Al anode XR50 source operating at 150 W. The detector used was a Phoibos MCD-9 Detector. The intrinsic error associated to the equipment was ± 0.1 eV of Binding Energy (BE).

The XPS analysis chamber was connected to a high-pressure chamber (HPC) where all the experiments were performed. The chamber was provided with an infrared lamp to increase the temperature and a thermocouple in contact with the sample holder that measured the temperature of the sample. The experiments were planned in order to avoid any contact between the solids and the atmosphere outside the XPS.

The treatment of the XPS spectra was done by using the CasaXPS program (Casa Software Ltd., UK). The reference peak was the O 1s, which was set at 529.7 eV. U $4f_{7/2}$ band was used to determine the uranium oxidation state. The band was deconvoluted into three different contributions, associated to U(IV), U(V) and U(VI), respectively, following the deconvolution methodology previously reported in Espriu-Gascon et al. [9].

Experimental methodology

Preliminary reduction of the UO_2 samples to stoichiometric UO_2

Initial UO_2 samples were determined to be partially oxidized due to their contact with atmospheric air and, in order to start the experiments with a stoichiometric UO_2, a pre-reduction process was needed. A previous study on the temperature needed to reduce the oxidized phases on non-doped UO_2 samples showed that the reduction was completed after 20 minutes of contact with H_2(g) (15 ml·min^{-1} of hydrogen from Messer (Germany) with 99.999% of purity) at 500ºC [9]. However, the necessary temperature to reduce uranium in the doped samples was 350ºC. This value was chosen to avoid melting the NPs and changing their size and properties. The determination of the oxidation state of uranium at the end of the pre-reduction step confirmed the complete reduction of uranium to U(IV).

Oxidation experiments with water vapor

Experiments were performed using a 15 ml/min of either argon or hydrogen stream from Messer (Germany) with 99.999% of purity. The gas flow was controlled by using a flow controller from MKS (USA). The gas was saturated with water vapor at room temperature and the gas mixture was introduced into the HPC chamber of the XPS to be in contact with the UO_2 samples. Once inside the reactor, the temperature was increased to the values shown in Table 1. Afterwards, the samples were cooled down and the gas mixture was pumped out from the HPC to reach vacuum conditions. Finally, the sample was transferred to the XPS analysis chamber avoiding any contact with the atmosphere.

As it can be seen in Table 1, two different series of oxidation experiments were carried out. In the first series, samples were put in contact with mixtures of argon and water vapor, and in the second series, argon was substituted by H_2(g).

Results and Discussion

Preliminary reduction of the UO_2 samples to stoichiometric UO_2

The non-doped UO_2 sample was previously reduced by hydrogen at 500 ºC, and the analysis of the surface showed that uranium was mainly U(IV). The U 4f XPS band showed the characteristics associated to U(IV) [17–20]: a Binding Energy of the U $4f_{7/2}$ band of 379.6 ± 0.1 eV (with a Full Width at Half Maximum (FWHM) of 2.0 eV) and a single satellite at 6.7 ± 0.1 eV from the U $4f_{5/2}$.

On the other hand, the preliminary reduction of the UO_2 doped with Pd nanoparticles was reached at 350 ºC; at this temperature, XPS spectra showed that uranium was actually U(IV). Considering that at 350ºC the non-doped UO_2 was not completely reduced [17] it seems that the presence of Pd nanoparticles in the UO_2 facilitates the reduction of the uranium on the surface.

Oxidation experiments carried out in the presence of argon and H_2O

Non doped UO_2

Table 2 shows the main characteristics of the U $4f_{7/2}$ band measured at the end of the experiments in the presence of argon and water vapor. From the deconvolution of this peak into the U(IV), U(V) and U(VI) bands, the oxidation state of the uranium in the surface of the solid night be calculated. The percentages of U(IV), U(V) and U(VI) are shown in Figure 1 at different temperatures. As it can be seen, at the three temperatures, uranium was actually oxidized, and the extent of oxidation increases with temperature. U(IV) percentage at 100ºC, 200ºC, and 350ºC were 57%, 42% and 7%, respectively. These results confirmed previous observations that temperature favored the extent of the oxidation of UO_2 by water vapor [5,9,21–23].

<u>UO_2 doped with Pd nanoparticles</u>

The characteristics of the $4f_{7/2}$ band of the surface of the solids at the end of the experiments carried out with doped samples are shown in Table 2. Figure 2 shows the percentages of U(IV), U(V) and U(VI) obtained by the deconvolution of the $4f_{7/2}$ band. On one hand, the percentage of U(IV) seems to be independent on the percentage of Pd nanoparticles and only a higher percentage of U(VI) than U(V) in the solid with a higher percentage of Pd nanoparticles should be mentioned. On the other hand, oxidation of the UO_2 increased with temperature, as in the non-doped UO_2 samples, and the percentages of U(IV) were similar at temperatures of 200ºC and 350ºC, independently on the presence of Pd nanoparticles. Both the characteristics of the $4f_{7/2}$ band and U(IV) percentages were very similar. This would indicate that the presence of Pd nanoparticles did not influence the process of UO_2 oxidation at such temperatures.

However, at 100ºC the results were different depending on the doping of the solid. As it can be seen in Figures 1 and 2, the percentage of U(IV) in the non-doped UO_2 was lower than 60% while in both experiments with doped UO_2, the surface of the solid presented percentages of U(IV) close to 100%. These observations reinforce the role of Pd in the UO_2

oxidation, showing that, at relatively low temperatures, Pd nanoparticles were able to inhibit the oxidation of UO_2 by water in the presence of argon.

Oxidation experiments carried out in the presence of H_2 and H_2O

The main result obtained in the experiments where doped UO_2 was exposed to H_2(g) saturated with water vapor was that the surface of the solid at the end of the experiments was composed of only U(IV), independently on the temperature. The U 4f XPS band obtained in all the experiments was characteristic of U(IV) and the U $4f_{7/2}$ band was located at a binding energy of 379.6 ± 0.1 eV, with a FWHM of 2.0 ± 0.1 eV.

This behavior was very different than the observed by Espriu-Gascon et al. [9] in the same experiments with H_2(g) and water vapor but without doping UO_2 with Pd nanoparticles. In such experiments, water vapor was able to oxidize the surface of the non-doped UO_2, (UO_2 surface at the end of the experiments contained less than 65% U(IV)) at the same temperatures than this work. The comparison between the percentage of U(IV) in both series of experiments (with no-doped and doped UO_2) can be seen in **Fig. 3**, where a consistent increase on the percentage of U(IV) is observed when the UO_2 was doped with Pd nanoparticles.

The main conclusion deduced from the reduced surface of the solids doped with Pd nanoparticles is that the presence of such particles completely avoided the oxidation caused by water vapor on the non-doped samples in the presence of H_2. It therefore emphasizes the importance of the presence in the SNF of epsilon particles and metallic precipitates consisting on Pd which would inhibit the oxidation of the fuel matrix if H_2(g) was present, retarding the oxidation and consequently dissolution of the fuel and the release of radionuclides to the environment.

Conclusions

The main conclusion of this work is related to the capacity of the epsilon particles or metallic precipitates to inhibit the oxidation of UO_2. The presence of such particles or precipitates was simulated in this work by depositing Pd nanoparticles in powdered UO_2.

On one hand, the presence of Pd nanoparticles on UO_2 facilitated the reduction by hydrogen of oxidized phases located on the UO_2 surface. On the other hand, avoided the oxidation of UO_2 by H_2O in the presence of H_2(g) in a range of temperatures between 100ºC and 350 ºC. In the presence of argon and water vapor, the oxidation of UO_2 was also inhibited at a relatively low temperature (100°C)

These conclusions indicate that epsilon particles and metallic precipitates located in the SNF could be critical on controlling the oxidation and reduction of the SNF matrix, and, by extension, the dissolution of the fuel and the release of radionuclides.

Acknowledgements

ENRESA and the Spanish Government (Ministerio de Economía y Competititvidad (MINECO), Spain) with the projects CTM2011-27680-C02-01 and ENE2014-54299-C2-1-R funded the work A. Espriu-Gascon wants to acknowledge the fellowship with reference code BES-2012-053098.

References

1. Smith R.E. (2011) Annotated Bibliography for Drying Nuclear Fuel, Idaho Falls, Idaho.

2. Higgs J.D., Lewis B.J., Thompson W.T., He Z. (2007) A conceptual model for the fuel oxidation of defective fuel, J. Nucl. Mater. 366:99–128.

3. Reed D.T., Van Konynenburg R.A. (1991) Effect of ionizing radiation on the waste package environment, in: High Lev. Radioact. Waste Manag., DCRL-JC--107180-Rev.l, DE91 015125, Lawrence Livermore National Lab., CA (United States), Washington, USA, pp. 1396–1403. https://www.osti.gov/scitech/biblio/138148 (accessed March 8, 2017).

4. Leenaers A., Sannen L., Van den Berghe S., Verwerft M. (2003) Oxidation of spent UO_2 fuel stored in moist environment, J. Nucl. Mater. 317:226–233.

5. MacCrone R.K., Sankaran S., Shatynski S.R., Colmenares C.A. (1986) Complex defects in the oxidation of uranium, Metall. Trans. A. 17:911–914.

6. Grambow B. (2010) Model Uncertainty for the Mechanism of Dissolution of Spent Fuel in Nuclear Waste Repository. Final MICADO Project report., European Commission.

7. Spahiu K., Werme L., Eklund U.-B. (2000) The influence of near field hydrogen on actinide solubilities and spent fuel leaching, Radiochim. Acta. 88:507–512.

8. Giménez J., Casas I., Sureda R., De Pablo J. (2012) Kinetics of hydrogen peroxide consumption in aqueous phase at different hydrogen partial pressures, Radiochim. Acta. 100:445–448.

9. Espriu-Gascon A., Llorca J., Domínguez M., Giménez J., Casas I., de Pablo J. (2015) UO_2 surface oxidation by mixtures of water vapor and hydrogen as a function of temperature, J. Nucl. Mater. 467:240–243.

10. Cui D., Low J., Sjöstedt C.J., Spahiu K. (2004) On Mo-Ru-Tc-Pd-Rh-Te alloy particles extracted from spent fuel and their leaching behavior under Ar and H_2

atmospheres, Radiochim. Acta. 92:551–555.

11. Kleykamp H. (1989) Constitution and thermodynamics of the Mo-Ru, Mo-Pd, Ru-Pd and Mo-Ru-Pd systems, J. Nucl. Mater. 167:49–63.
12. Cui D., Low J., Rondinella V.V., Spahiu K. (2010) Hydrogen catalytic effects of nanostructured alloy particles in spent fuel on radionuclide immobilization, Appl. Catal. B Environ. 94:173–178.
13. Ferry C., Poinssot C., Broudic V., Cappelaere C., Desgranges L., Garcia P., Jégou C., Lovera P., Marimbeau P., Corbel C., Miserque F., Piron J.P., Poulesquen A., Roudil D., Gras J.M., Bouffioux P. (2005) Referentiel scientifique sur l'evolution a long terme des combustibles usés. Commissariat à l'Energie Atomique (CEA) Technical Report RT DPC/SECR 04-032 (March 2005).
14. Shoesmith D.W. (2008) The role of dissolved hydrogen on the corrosion / dissolution of Spent Nuclear Fuel. Report NWMO TR-2008-19, Ontario, Canada.
15. Serrano-Purroy D., Clarens F., González-Robles E., Glatz J.P., Wegen D.H., de Pablo J., Casas I., Giménez J., Martínez-Esparza A. (2012) Instant release fraction and matrix release of high burn-up UO_2 spent nuclear fuel: Effect of high burn-up structure and leaching solution composition, J. Nucl. Mater. 427:249–258.
16. Espriu-Gascon A., Bastos-Arrieta J., Giménez J., Casas I., de Pablo J. (2016) Preparation and characterisation of Pd nanoparticles doped UO_2 samples, Int. J. Nanotechnol. 13:627–633.
17. Stumpf S., Seibert A., Gouder T., Huber F., Wiss T., Römer J. (2009) Development of fuel-model interfaces: Investigations by XPS, TEM, SEM and AFM, J. Nucl. Mater. 385:208–211.
18. Van den Berghe S., Laval J.-P., Gaudreau B., Terryn H., Verwerft M. (2000) XPS

investigations on cesium uranates: mixed valency behaviour of uranium, J. Nucl. Mater. 277:28–36.

19. Allen G.C., Tempest P.A., Tyler J.W. (1987) Oxidation of Crystalline UO_2, studied using X-Ray Photoelectron Spectroscopy and X-Ray Diffraction, J. Chem. Soc. Faraday Trans. 1. 83:925–935.

20. Idriss H. (2010) Surface reactions of uranium oxide powder, thin films and single crystals, Surf. Sci. Rep. 65:67–109.

21. Hedhili M.N., Yakshinskiy B. V, Madey T.E. (2000) Interaction of water vapor with UO_2 (0 0 1), Surf. Sci. 445:512–525

22. Senanayake S.D., Idriss H. (2004) Water reactions over stoichiometric and reduced UO_2(111) single crystal surfaces, Surf. Sci. 563:135–144.

23. Senanayake S.D., Rousseau R., Colegrave D., Idriss H. (2005) The reaction of water on polycrystalline UO_2: Pathways to surface and bulk oxidation, J. Nucl. Mater. 342:179–187.

Figure Captions

Fig. 1 Composition of the surface of non-doped UO_2 at the end of the oxidation experiments with argon and water vapor. The percentages of the different oxidation states were calculated from the deconvolution of the U $4f_{7/2}$ band.

Fig. 2 Uranium oxidation state in the surface of the solids in the experiments in the presence of argon and water vapor. UO_2 doped with (A) 0.5% wt. Pd nanoparticles, and (B) 1.5% wt. Pd nanoparticles.

Fig. 3 U(IV) percentage in the solid surface at the end of the experiments carried out in the presence of $H_2(g)$ and water vapor.

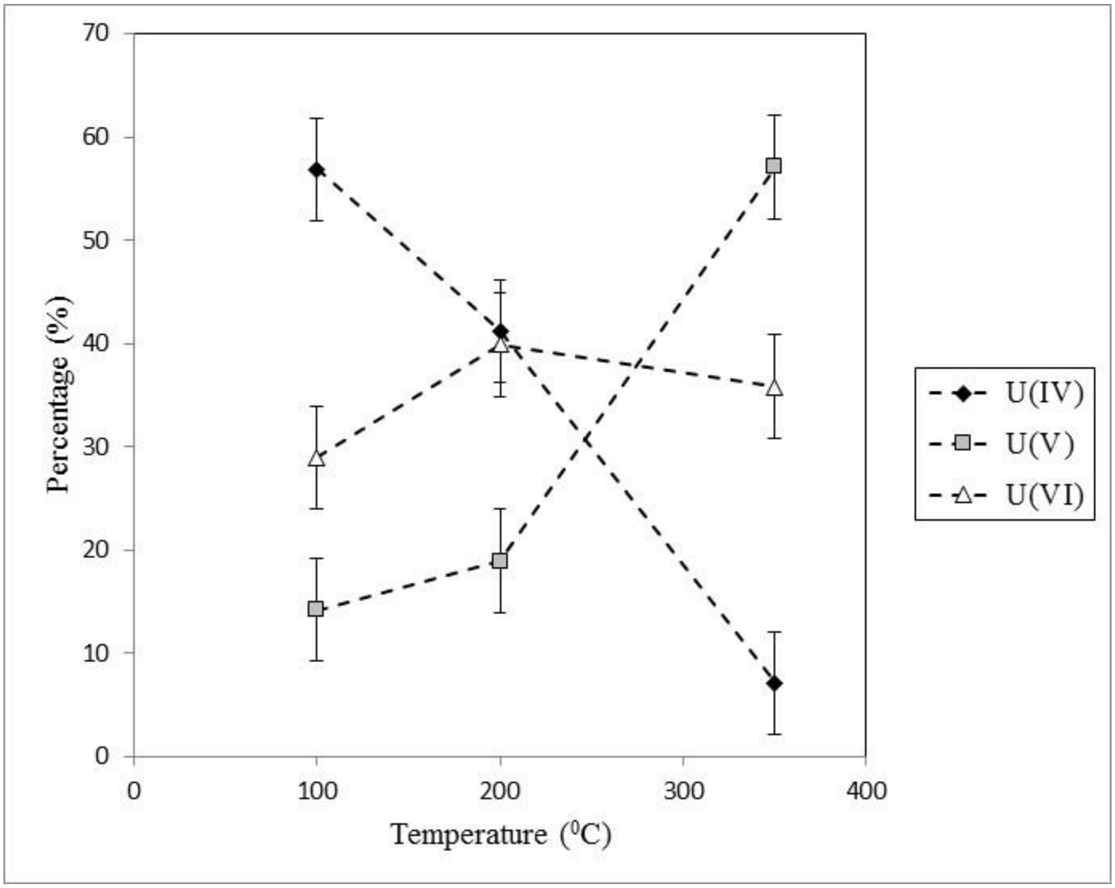

70
60
50
40
30
20
10
0
0
100
200
300
400
Percentage (%)
Temperature (⁰C)
U(IV)
U(V)
U(VI)

Fig. 1

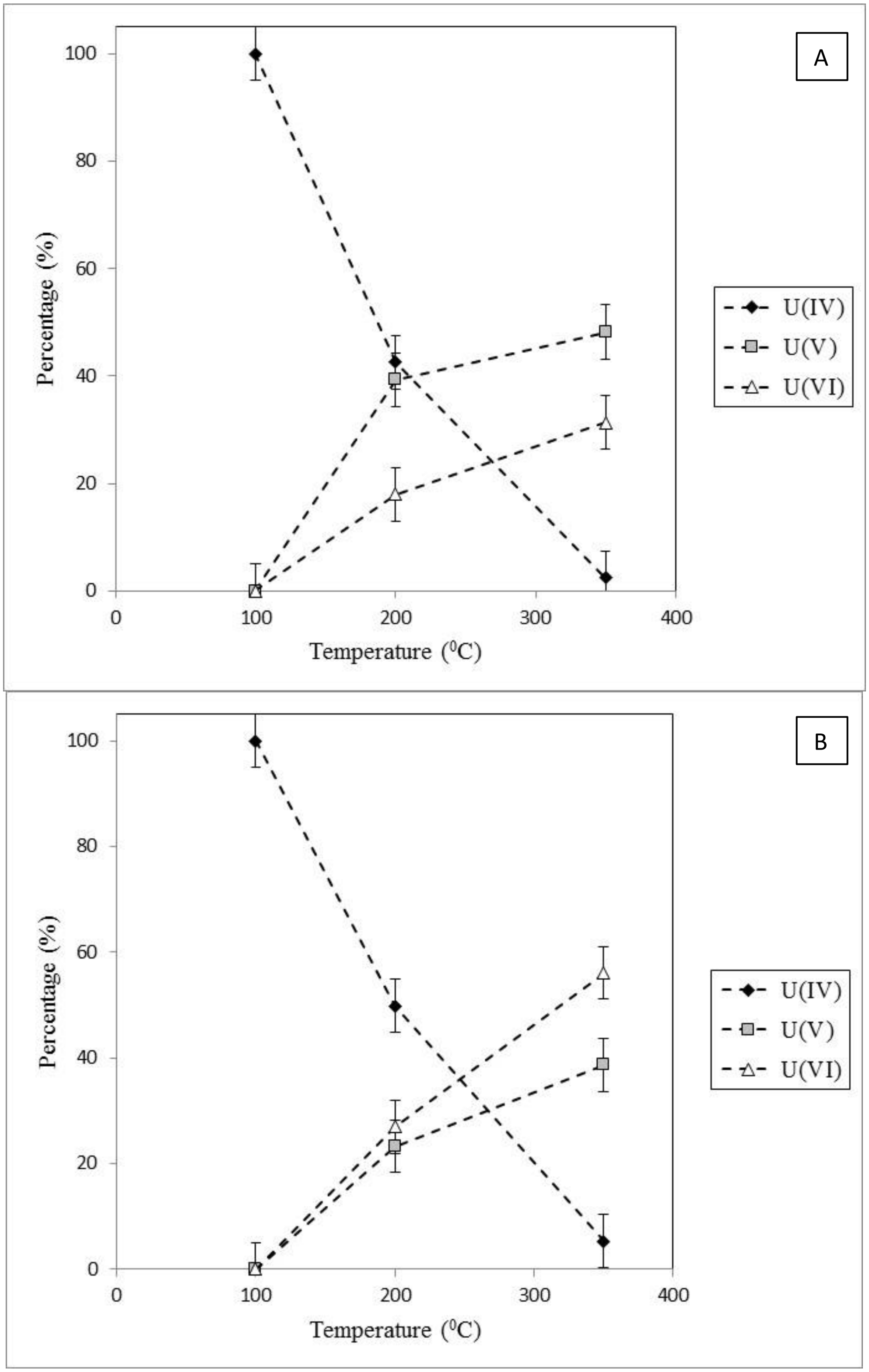
A
Percentage (%)
Temperature (⁰C)
U(IV)
U(V)
U(VI)
B
Percentage (%)
Temperature (⁰C)
U(IV)
U(V)
U(VI)

Fig. 2

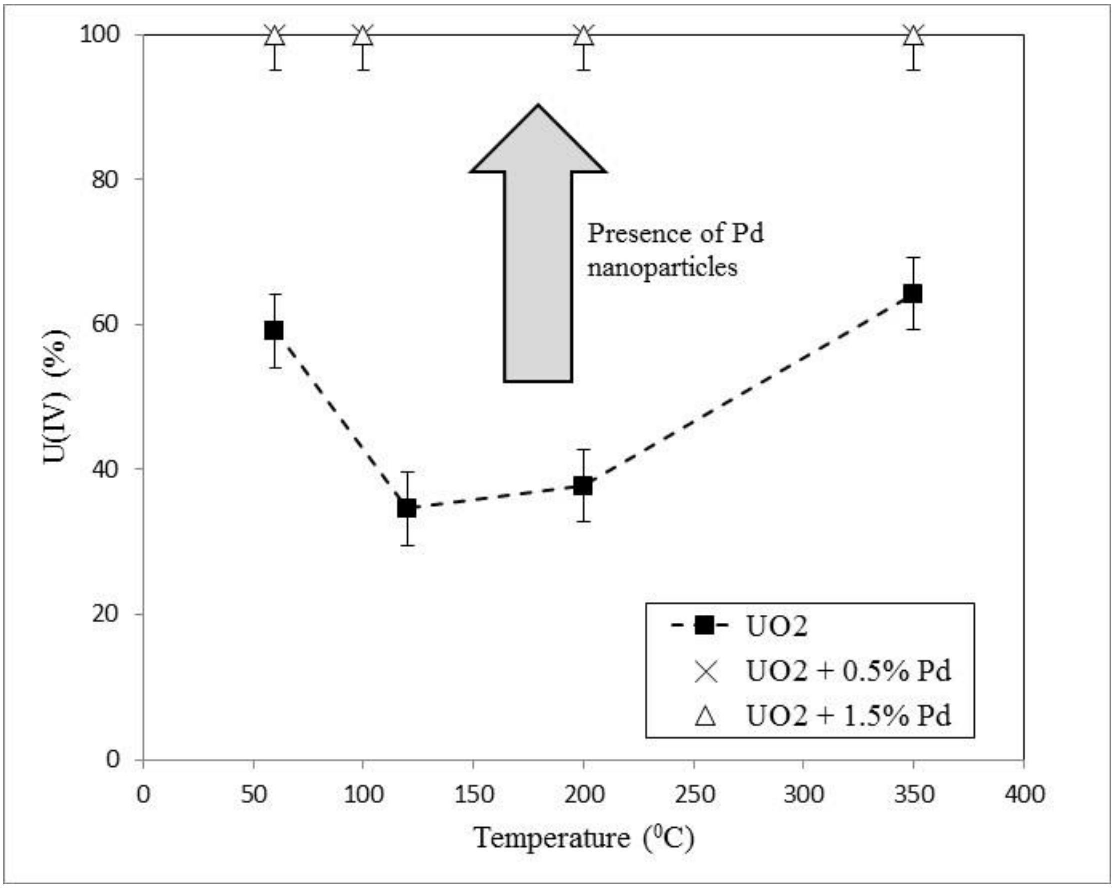
100
80
60
40
20
0
U(IV) (%)
Presence of Pd
nanoparticles
UO2
UO2 + 0.5% Pd
UO2 + 1.5% Pd
0
50
100
150
200
250
300
350
400
Temperature (0C)

Fig.3

Table 1 Experiments carried out in this work with the three samples (non-doped UO_2, UO_2 doped with 0.5 % of Pd nanoparticles, and UO_2 doped with 1.5 % of Pd nanoparticles). The flow rate of the gas mixtures was always 15 ml/min.

Experiment	Gas	H_2O vapor	Temperature (ºC)	Time (minutes)
T-H_2 (350)	H_2	No	350	20
T-H_2 (500)	H_2	No	500	20
T-Ar H_2O (100)	Ar	Yes	100	10
T-Ar H_2O (200)	Ar	Yes	200	10
T-Ar H_2O (350)	Ar	Yes	350	10
T-H_2 H_2O (60)	H_2	Yes	60	10
T-H_2 H_2O (100)	H_2	Yes	100	10
T-H_2 H_2O (200)	H_2	Yes	200	10
T-H_2 H_2O (350)	H_2	Yes	350	10

Table 2 Characteristics of the U 4f XPS band obtained after performing the experiments in mixtures of argon and water vapor. All the measurements are in eV and the satellite positions refer to the U $4f_{5/2}$ band.

Experiment	**BE U$4f_{7/2}$**	**FWHM U$4f_{7/2}$**	**ΔBE satellite 1**	**ΔBE satellite 2**
Non-doped UO_2				
Ar+H_2O, T=100ºC	379.8	2.4	6.5	8.3
Ar+H_2O, T=200ºC	380.0	2.6	6.1	8.0
Ar+H_2O, T=350ºC *	380.5	2.6	5.5	8.2
UO_2 + 0.5% Pd				
Ar+H_2O, T=100ºC	379.6	2.0	6.7	
Ar+H_2O, T=200ºC	379.8	2.4	6.5	8.5
Ar+H_2O, T=350ºC	380.3	2.5	6.3	8.1
UO_2 + 1.5% Pd				
Ar+H_2O, T=100ºC	379.6	2.0	6.7	
Ar+H_2O, T=200ºC	380.1	2.5	6.1	8.1
Ar+H_2O, T=350ºC	380.6	2.4		7.7

* *Espriu-Gascon et al.* [9]

Table 3 Characteristics of the U 4f XPS band obtained after performing each experiment with a 0.5 wt % Pd doped sample. All the measurements are in eV and the satellite positions are referred to the U $4f_{5/2}$ band.

Experiment	**BE U4f$_{7/2}$**	**FWHM U4f$_{7/2}$**	**ΔBE satellite 1**	**ΔBE satellite 2**
Non-doped UO_2*				
H_2+H_2O, T= 60ºC	379.9	2.5	6.5	9.0
H_2+H_2O, T= 120ºC	380.3	2.6	5.8	8.5
H_2+H_2O, T= 200ºC	380.1	2.6	5.9	8.5
H_2+H_2O, T= 350ºC	379.8	2.4	6.4	9.1
UO_2 + 1.5% Pd				
H_2+H_2O, T= 60ºC	379.6	2.0	6.7	
H_2+H_2O, T= 120ºC	379.6	2.0	6.7	
H_2+H_2O, T= 200ºC	379.6	2.0	6.7	
H_2+H_2O, T= 350ºC	379.6	2.0	6.7	

* *Espriu-Gascon et al.* [9]